Journal of Intelligent & Robotic Systems (2021) 102: 3
https://doi.org/10.1007/s10846-021-01359-5

SHORT PAPER

MeWBots: Mecanum-Wheeled Robots for Collaborative Manipulation in an Obstacle-Clustered Environment Without Communication

Aditya Rauniyar[1] · Hem Chandra Upreti[1] · Aman Mishra[1] · Prabhu Sethuramalingam[1]

Received: 22 January 2020 / Accepted: 1 March 2021 / Published online: 13 April 2021

Abstract

This paper presents a displacement based collaboration strategy to carry a payload greater than the robot's limit and transport it to a desired location through a planar cum obstacle-clustered environment using a multi-robot system. The proposed model has no explicit communication between the robots but it is verified that local measurements received from the payload's motion data can be used as implicit information to drive the robot. A leader robot (manually controlled) guides the follower robot (fully autonomous) with load clamped on both robots. The follower robot computes a coordinated obstacle-avoidance motion based on the input variables received from its sensors. Due to the defined need to navigate narrow pathways quickly and easily, the current study approach advocates the deployment of Mecanum-Wheeled Robots (MewBots). The kinematic simulations clearly depict their capability to translate in any direction without changing their orientation. Using this information, an experimental model is prepared by deploying a strategy devised to perform a collaborative manipulation in four environmental cases.

Keywords Omni-directional robots · Multi-robot system · Collaborative manipulation

1 Introduction

Mobile robots have found application in diverse fields ranging from hospital assistance, to delivery of goods to specific locations. One of such applications includes transporting the goods in a warehouse, mainly by using Automated Guided Vehicles (AGVs). These warehouse mobile robots bring in a stack of products from distant locations to the packaging area. These products are generally small in size and can be put up on a rack. However, a difficulty arises when the task involves objects that have characteristics beyond the handling capacity of these robots (such as, larger, heavier and non-uniform objects). In this scenario, either a bigger and more powerful robot must be used or the task can be effectively completed by the collaboration of multiple mobile robots. The problem with the former option is that different systems will be needed for each specific purpose which makes the overall automation procedure uneconomical. Additionally, a larger system means that it would be difficult to maneuver narrow and curved pathways. On the other hand, the latter concept of a collaborative system has been proven by several studies to be a versatile and more economical technique (e.g. 20, 26, 31, 32), making it an emerging domain.

For a collaborative system, there must either be explicit communication between robots or different motions of individual robots must be computed based on the implicit information received from the local measurements. In either of these cases, the following approaches can be adopted: Centralized approach, wherein one robot among the system of robots will have the commanding power to guide and control the overall proceedings and will be responsible for containing the core algorithm, whereas in decentralized approach each robot will be accountable for maintaining the overall control architecture for a collaborative manipulation. These two techniques have their individual merits and challenges. Nonetheless, communication is complicated in these systems, as it requires separate algorithms, hardware and wiring. These have proved to affect performance due to latency and limited bandwidth capability, as stated by earlier

✉ Aditya Rauniyar
mail.adityarauniyar@gmail.com

[1] Department of Mechanical Engineering, SRM Institute of Science and Technology, Chennai, Tamil Nadu 603203, India

research studies [21, 33]. Hence, to reduce complexity and achieve redundancy, the development of systems without explicit communication must be preferred. Additionally, when a system is independent of such communication, there is no need to state the number of robots in a collaborative system, as noted by [31]. Hence, it may be concluded that designing an appropriate architecture with only the local measurements of mounted sensors is a better and more economic] alternative.

This research paper presents a displacement-based coordination approach to facilitate the appropriate information required by individual robots to compute their motion. These sets of data can be attained when robots are equipped with necessary sensors at each clamping joint of the robots to clamp the shared payload. In this strategy, two robots: "Leader" and "Follower" are presented. The leader can be a human or can be a remotely controlled robot, as long as a guiding force to another robot is provided. The follower robot is fully autonomous and goal-centric. These robots are required to carry a payload and bring it to a specified location through an obstacle clustered environment with no explicit communication and only based on local measurements. Due to their unique ability to navigate narrow paths without changing orientation, four Mecanum-Wheeled Robot (MeWBot) are selected for this operation.

The kinematics of the MeWBot are derived with assistance from [29]. These wheels provide an unconstrained directional motion to the overall cooperative manipulation. The remotely controlled leader robot is the only one facilitated with the information of the global destination and is manually guided to reach that point. On the other hand, the follower robot is uninformed about the final position. Furthermore, a key aspect of making a mobile robot autonomous is by adding an obstacle-avoidance capability to it. Hence, the follower robot computes a coordinated obstacle-avoidance motion based on the leader force. The payload clamped on these robots is used to transmit the leader force to the follower robot. An additional degree of freedom is provided as a constrained relative motion between the payload and the follower robot towards the applied force. This force is sensed as a direct co-relation to displacement produced on this DoF. A visualization of this set-up can be seen in Fig. 1.

The rest of the paper is organized as follows: a detailed background and related work are discussed, followed by the adopted methodological approach. In this section, the basic assumptions of the study are presented. Additionally, the system is formulated into four specific cases, which are further elaborated. The proposed coordination architecture of the collaborative manipulation and the follower robot's control algorithm are described under it. Furthermore, Kinematic formulation of the MeWBot is stated and the quantified overall system is represented mathematically. Thereafter, a system overview of the leader and follower robots is presented. Furthermore, a SIMULINK model of the MeWBot is attached, followed by the simulation results. Finally, the experimental results are tested based on the specific cases under problem formulation. Lastly, the conclusions of the study and scope for extending the work further in future are discussed.

2 Comprehensive Literature Review of Related Work

The need for multi-tasking systems has necessitated the use of collaborative manipulation. To fully understand the benefits of coordinated performance, inspiration can be drawn from nature. An earlier research work [7] has presented a study on a group of ant species indicating the contribution of individual ants to the transportation of food from one location to another. Ants do not know the weight of any load that has to be lifted but depending upon the weight their numbers multiply until movement is possible, which was presented in the paper through the depiction of a quasi-static model of planar manipulation. Additionally, [4] presented a novel concept to relocate vehicles by lifting and transporting via a system of coordinated robots. This

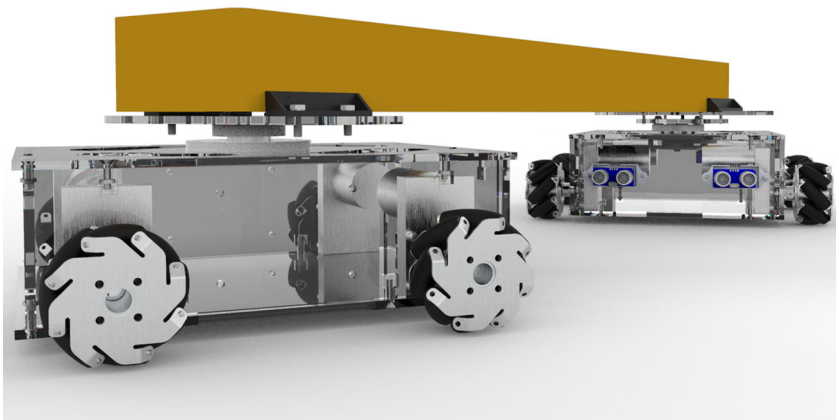

Fig. 1 The remotely controlled leader robot(left) guides the fully autonomous follower robot(right) with a payload clamped on both of them. The follower senses the force through the payload and computes an obstacle-avoidance trajectory

was made possible by initially scanning the environment by a centralized system and with motion planning, this system remotely monitored each step made by the extraction robots. Furthermore, collaborative systems have also found application in the assembly domain, as shown by an earlier research work [20]; the domain used heterogeneous robots divided into two tasks: parts delivery and parts assembly, to put together a table. It had an automatic assembly sequence generator and a unique torque gripper to complete the task.

To make this cooperative manipulation come to life, two types of communication takes place between the robots or systems: explicit communication and implicit communication. The first one used by [26] presents a parallel manipulation using leader and follower concept, where a leader communicates with the follower robots to move a sofa, controlling both the position and orientation. However, this tends to produce noise, packet losses and time-varying delays, as stated in [33]. Another study [21] added to the flaws of explicit communication by presenting the average consensus problem associated with it. Hence, of late, more focus has been given to implicit communication based on local measurements. For instance, in one study [31], the robots were solely guided by the onboard sensors receiving signals from the leader robots' motion through the payload (used as a medium of force transmission). The three-follower robots were used to amplify the force on the object to in the direction in which the leader robot (manually or autonomously controlled) pulled/pushed using a Force-ANTS technique.

In addition, the computational performance depends on both centralized and decentralized approaches. Mostly, the centralized approach advocates explicit communication, as detailed in [26]. Therefore, assigning robots to make their own decision based on sensory inputs is more common now, as detailed in several research studies (e.g. 6, 9, 13, 14, 24, 31 and 12). This approach, however, has dynamic challenges, as explained by [14]; the noise associated with object velocity measurements and each robot gets incorporated with this implicit decentralized approach.

Furthermore, the type of object dealt with can be categorized as rigid and deformable objects. Rigid bodies are more commonly used and consequently, there are more research studies on them (e.g. 8, 13, 24, 26, 31 and 12). Moreover, efforts have been put forth by [3] and [20] to manipulate deformable objects (Like a blanket) using shape maintenance approach. Here, each robot senses the force exerted by the object to the robot's end effector and computes a collision avoidance trajectory to reach force equilibrium.

For proper positioning of a robot and object, it is necessary to understand and derive the kinematics of the full system, as done by [25]. However, precise kinematic positioning is not possible. Hence, when mobile manipulators tend to collaborate to move a designated object, stress is observed to develop between the robotic manipulator and the object due to kinematic errors. Therefore, to reduce or negate this flaw, Erhart et al. [11] presented an impedance-based coordination for kinematic uncertainties while using heterogeneous manipulators.

Additionally, there exists various types of controllers that have shown promising results. One such is the potential field-based controller first introduced by [24], it uses tens to thousands of mobile robots to trap and transport an object. A potential field is assigned to each of these robots to ensure that they do not collide with one another during the coordinated transport. Similarly, Esposito [12] provided a methodology named "artificial potential field" to control the velocity of an object by force. Moreover, coherent robot behavior based on local information through a simple neural controller was studied by [6]. Additionally, specific theories like Lyapunov stability theory, and graph theory along with Recompile fuzzy-sliding mode control were emphasized by [19] and [9]. It is also plausible to incorporate a trap and transport-based control scheme, as shown by [8, 13, 18]. Furthermore, Amato et al. [5] presented the decision planning for a multi-task multi-robot system to reduce uncertainty in command execution and achieve a collaborative effort. Exploring the plausibility of fuzzy-controlled systems, Teixeira et al. [15] used visual and laser fuzzy-feedback with a centralized system to keep the overall system coordinated and collision-free, these robots were well-aware of their environment and were capable of complicated maneuverability.

As stated by [31], an omnidirectional robot platform provides better mobility as it is not limited by the non-holonomic constraint and can therefore achieve more accurate 2D force feedback control. A novel custom-designed platform using four omni-wheeled robots called as "OuijaBot" was discussed by [20]. The study adopted a decentralized approach with no explicit communication and successfully achieved translation and rotation control of the object (i.e., long slab) to be transported. Therefore, there is more focus on omni-directional robots for the chosen application of the current study.

Different mobile robots are continually being designed and constructed to increase the pace of mass production and to lower production costs and increase efficiency as discussed by [17]. There is an increased demand for high-performance mobile robots in terms of locomotion and accuracy, and Mecanum wheels have been found capable of boosting efficiency [23]. Another research work found [28] that the omnidirectional mobile platform could move instantaneously in any direction from any configuration. The study explained that the omni-directional feature of the Mecanum wheels allowed the robot to move in any direction without changing its orientation. The advantage of this platform is that a robot can easily cover a certain distance in lesser time compared to a conventional robot.

This improves its performance in congested environments and narrow passages such as those commonly found in-factories, industries, warehouses, and hospitals. A good example is the autonomous Mecanum wheeled vehicle developed for the autonomous cleaning of the Dubai international airport roof [27].

The structure and formation of the wheel in a Mecanum wheeled robot is in such a way that it has the potential to move through a different path which can be either a plain or deflected path. A mobile omni-directional platform (KUKA youBot) with two pairs of coaxial Mecanum wheels, on the periphery of each of which were mounted six rollers, the axis of which were skewed with the axis of the wheel at the angle of 450, was explained in the study undertaken by [1, 5] and [28]. The rollers placed in the wheel helped to slide the robot diagonally. These rollers helped in the movement of each diagonal wheel towards a sliding direction. Gfrerrer [16] Mecanum wheeled omnidirectional mobile robots can move along coordinates and do not require any steering system. Due to such coordinate movement, the robots can move in narrow paths where agile manipulation is needed. To implement these features, the Mecanum wheeled robot requires an advanced control system to control both the position and orientation. The efficiency of a mobile robot also depends on the wheel geometry and developing it along with the connection to the platform helps in the control of these types of models.

Mecanum-wheeled robots were noted by [2] to have a superior advantage in terms of mobility in narrow spaces and crowded environments. These robots are suitable for working in factory workshops, warehouses, hospitals and other such environments. They have the ability to perform tasks in both static as well as dynamic obstacle-clustered environments. In addition, Voinescu et al. [30] provided methods to make Mecanum wheeled robots versatile enough to adapt to any scenario. Due to slip and uneven reaction forces on an uneven platform, Doroftei et al. [10] presented a four-passive suspension Mecanum wheeled robot with obstacle avoidance capability using a sonar and camera. Furthermore, Padgett and Browne [22] presented a vector-based avoidance algorithm which used LiDAR and Mecanum robots. The study verified that due to the vector-based output and mobility of LiDAR and Mecanum robots, respectively, integration of these robots was much easier than other conventional systems.

All in all, cooperation and coordination were proved to be very beneficial in all sectors. Likewise, drawing inspiration from the coordinated transport strategies evident in nature (viz. ants), it is plausible to delimit what can be achieved from a single system. Many research studies have focused on exploring the applicability of this very technique and promising results have been obtained for attempts to reduce the complexity in a coordinated system. Notable among these is the use of non-communicative decentralized strategies along with omni-directional system if the robot is to traverse narrow and complicated trajectories. Recently emerging research in this field has been of coordinately dealing with flexible payloads. However, when considering several real-life applications, more focus has been on handling rigid payloads. Although dealing with rigid payloads requires less knowledge of their dynamic properties, the computed kinematics of the system are affected due to stress development. Up till now, these practical scenarios have been handled with a feedback-controller in relation to the system and the environment.

3 Collaborative MewBots

Motivated by the work done by [32] and [31], who introduced and analyzed the approaches and challenges associated with collaborative systems, the current study advocates the deployment of four Mecanum wheeled robots called as “MeWBot”, with their forward and inverse kinematics derived from the earlier study conducted by [29]. The present study derives inspiration from the natural behavior of ants who are capable of collectively lifting weights much higher than their individual weight. The methodology is based on a scenario where person “A” guides a person “B” by holding his hand, wherein person “B” moves in proportion to the magnitude of the pull towards the direction indicated by person “A”. Using this, the current study attempts to put forth a collaborative method to carry and transport objects using MeWBots.

4 Kinematic Representations

4.1 Kinematic Formulation of MeWBot

The MeWBot equipped with Mecanum wheels has a passive roller placed at an angle of 45° with respect to the wheel axis. When each of the wheels is actuated, these rollers tend to provide a reaction force in a direction normal to the roller axis, as shown in Fig. 2 with green vector arrows. The summation of these forces produced by each wheel provides the robots with an overall direction of motion. Consider the following notation for gaining a better understanding:

- YGX as the global coordinate frame.
- $Y_R O X_R$ as the robot’s coordinate frame.
- $(\omega_1, \omega_2, \omega_3, \omega_4)$ be respective wheel velocities in $rads^{-1}$.
- R be the radius of wheel in $meters$.
- ω_Z be the angular velocity about an axis perpendicular to both X_R and Y_R in $rads^{-1}$.
- V_x be the translation velocity of the robot in X_R direction in ms^{-1}.

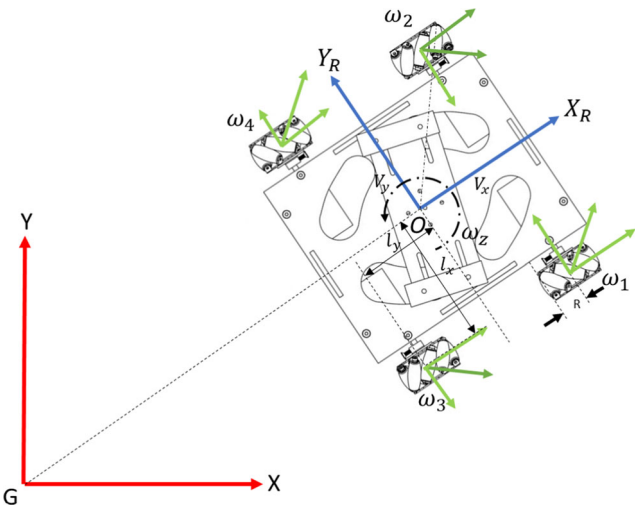

Fig. 2 Wheel configuration and parameters of the Four Mecanum Wheeled Robot

- V_y be the translation velocity of the robot in Y_R direction in ms^{-1}.
- l_x be half the track width in $meters$.
- l_y be half the wheelbase in $meters$.
- R^F be the denotation for follower robot.
- R^L be the denotation for leader robot.

$$\begin{bmatrix} V_x \\ V_y \\ w_z \end{bmatrix} = \frac{R}{4} \begin{bmatrix} 1 & 1 & 1 & 1 \\ -1 & 1 & 1 & -1 \\ \frac{-1}{(l_x+l_y)} & \frac{1}{(l_x+l_y)} & \frac{-1}{(l_x+l_y)} & \frac{1}{(l_x+l_y)} \end{bmatrix} \begin{bmatrix} w_1 \\ w_2 \\ w_3 \\ w_4 \end{bmatrix} \quad (1)$$

$$\begin{bmatrix} w_1 \\ w_2 \\ w_3 \\ w_4 \end{bmatrix} = \frac{1}{R} \begin{bmatrix} 1 & -1 & -(l_x+l_y) \\ 1 & 1 & l_x+l_y \\ 1 & 1 & -(l_x+l_y) \\ 1 & -1 & l_x+l_y \end{bmatrix} \begin{bmatrix} V_x \\ V_y \\ w_z \end{bmatrix} \quad (2)$$

4.2 Collaborative System Kinematics

The follower robot, R^F rests on the background of the constrained parameters. Due to the limits of the preferred sensors, there is a minimum and maximum value for θ, denoted by θ_{min} and θ_{max} respectively, as shown in Fig. 3. The magnitude of force **F** produced by the motion of the leader robot on the payload is sensed by the follower robot in direct proportion to the degree of displacement produced, as shown in Eq. 3 below:

$$d = f(\mathbf{F}) \quad (3)$$

The direction of this force is given by θ. Using these two inputs, the robot's velocities (V_{xf}, V_{yf}), can be calculated as follows:

$$V_{xf} = d\cos\theta \quad (4)$$

$$V_{yf} = d\sin\theta \quad (5)$$

The robot moves along the **F** until an obstacle hinders its path or until it reaches either θ_{min} or θ_{max} position. During this change in θ, the robots' orientation must compensate for this alteration. Hence, ω_Z is introduced as a function of θ, as shown in Eq. 6 below.

$$\omega_z = \theta e^{e^{|\theta|}-c} \quad (6)$$

5 System Overview

In order to verify this displacement-based collaborative theoretical model, two robots are built with different configurations. These robots are used to take input commands from the user, sense forces as per displacement and compute

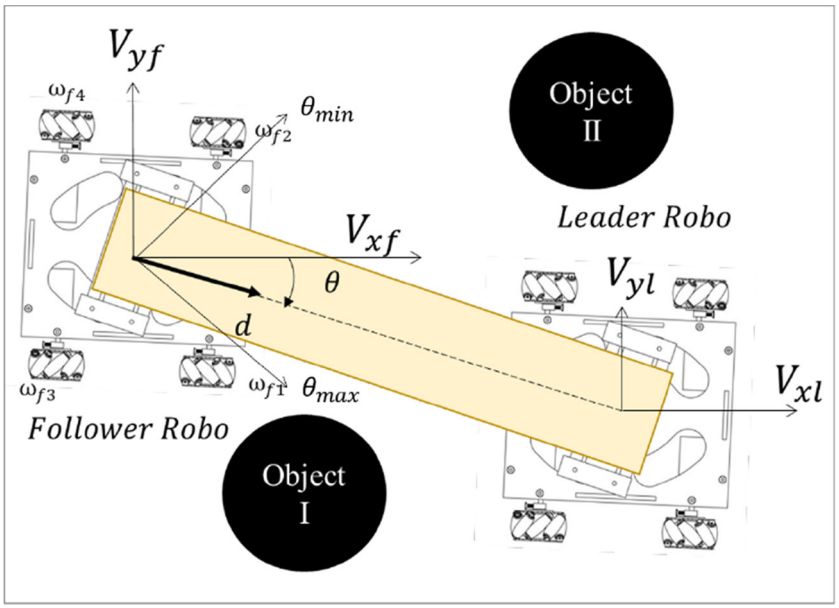

Fig. 3 Schematic representation of proposed collaborative system in an obstacle-clustered environment. The on-board sensor on the follower robot senses leader robot's force in terms of displacement(d) and angle(θ). The angle sensor on the follower robot has a limit from θ_{min} to θ_{max}

obstacle-avoidance coordinated trajectories. With the development of these robots, the robustness of the Mecanum-wheeled robots for collaborative manipulation is demonstrated. These robots are designed right from scratch and are kept as simple as possible with the consideration of minimal overall cost. Modern manufacturing techniques are employed to accomplish the proposed design.

5.1 Leader Robot

5.1.1 Mechanical Design

The body of the MeWBot leader is made of a 4mm thick acrylic sheet. Each of the parts is designed and machined using laser cutting operation. The parts are assembled together using slots along with bolts and nuts. The Mecanum wheels with 3 inches diameter for 10mm (approx.) ground clearance is also designed using software. It consists of 10 parts: 2 wheels and 8 rollers. These wheels and rollers are 3D printed using PLA material and are then assembled using Allen bolts. To improve traction between the rollers and the ground surface, heat shrink of polyolefin material is applied to the rollers. Additionally, flange couplings are custom-designed for the wheels and motors, and machined through lathe operations. The upper platform is a turntable mechanism containing thrust bearings and 3D printed mounts. Furthermore, clamping jaws are provided on the turntable to hold the payload intact, as shown in Fig. 4.

5.1.2 Control Architecture

Figure 5 shows the control architecture of the leader robot. It consists of a Wi-Fi development kit called as Wemos D1 mini running at 80MHz with ESP8266 chip. The leader robot is remotely controlled from a mobile phone using Blynk App, as seen in Fig. 9. The app contains two analog joysticks which control the translation and rotation of the robot, respectively. Wemos, containing a Wi-Fi module also has a few input-output pins. These are used to signal two

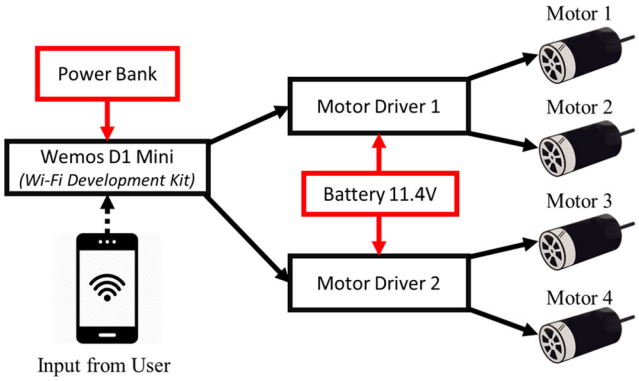

Fig. 5 Control and power layout of leader robot

channel motor drivers powered by a Li-Po batter of 11.4V. A power bank is used to power the development kit. Therefore, based on the user's input through the analog sticks, the leader robot moves in the same direction with given velocity using Eq. 2. Four 78 kg-cm rectangular gear box motors are used for this purpose.

5.2 Follower Robot

5.2.1 Mechanical Design

The follower robot's main body and wheel assembly are similar to that of the leader robot, the difference being that it is equipped with more sensors and their mounts. In the front acrylic sheet, there are 3D printed mounts for ultrasonic sensors inclined at an angle of 60°, as shown in Fig. 6. The upper turntable has an additional constrained degree of freedom in a linear direction towards the leader robot's force. Furthermore, the turntable is coupled with a pair of spur gears in 1:2 ratio to sense the angle at which the R^L applies force. Hence, both the magnitude (d) and direction of the force (θ) are sensed in this manner, which can be] seen in the assembly displayed in Fig. 7.

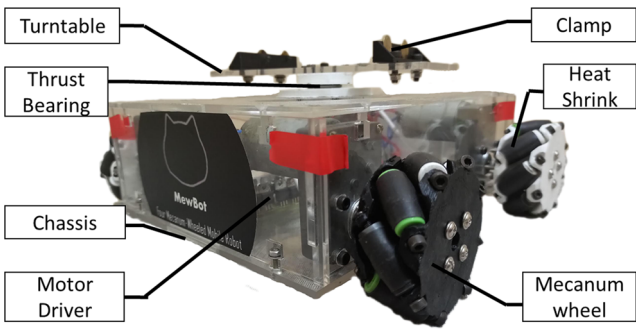

Fig. 4 Custom designed and manufactured leader robot with key components labeled

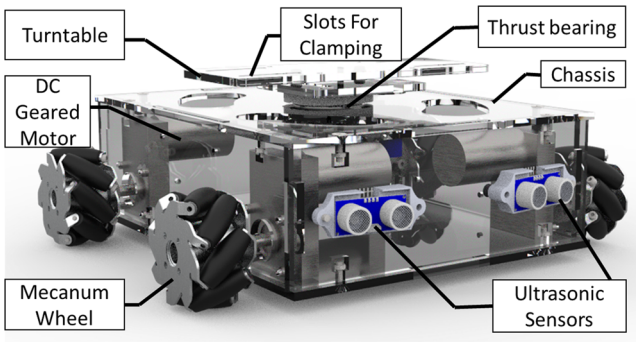

Fig. 6 Custom designed and manufactured follower robot with appropriate sensors for full autonomy

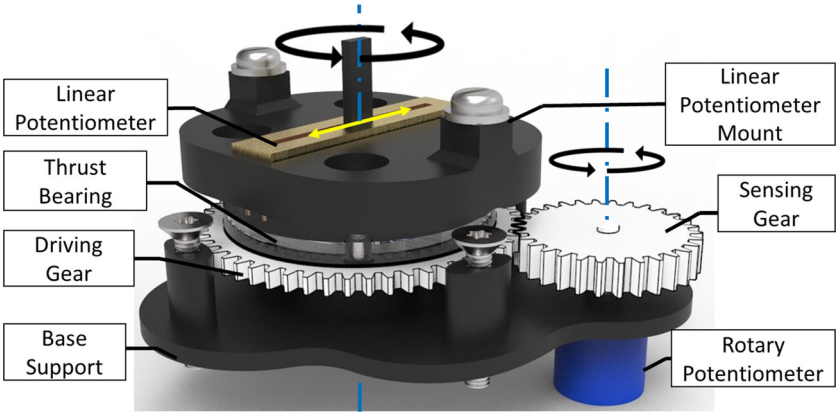

Fig. 7 Hardware assembly for sensing a displacement based force from leader robot. Liner potentiometer is used to sense d whereas rotary potentiometer senses θ

5.2.2 Control Architecture

Figure 8 displays the overall control structure of the follower robot. The ultrasonic sensor is mounted in an inclined fashion so to detect obstacles in the forward-right and forward-left positions of the robot. Additionally, the upper platform contains a 40mm B50KΩ slide potentiometer, arranged such that the slide is along the direction of force of the leader robot. The turntable is coupled with a 10KΩ rotary potentiometer through a pair of spur gears, as shown in Fig. 6. All these are sensed by an Arduino UNO running at 16MHz. It computes an obstacle-avoidance trajectory and feeds signals to two two-channel L293n motor drivers using Eq. 2. These drivers are powered with a 11.4V Li-Po battery. Four 78 kg-cm rectangular gear box motors are used for this purpose.

6 Methodology

6.1 Assumptions

For a collaborative manipulation of the multi-robot (or two robots) system, the leader R^L and follower R^F robots are used to carry and transport payload" through an environment with "O_i" Objects. The following assumptions are considered in order to successfully test the collaborative strategy put forth using these robots:

Assumption 1 R^L and R^F receive the payload, W in a way such that the transverse mid-plane of the payload aligns with the transverse mid-plane of the two robots.

Assumption 2 It is assumed that the clamps used to hold this weight have no backlash. In other words, there exists no relative motion between the clamps of the leader and follower robots.

Assumption 3 The payload is rigid in a manner where the motion of the leader robot is instantly sensed by that of the follower robot, indicating that payload has no strain due to R^L's motion or during the coordinated task.

Assumption 4 Obstacles O_i are placed in orientation such that they are detected by the R^F, if there is a need to perform obstacle avoidance.

Assumption 5 Wheel slip, either in R^L or R^F, has no effect on the overall maneuverability of the system.

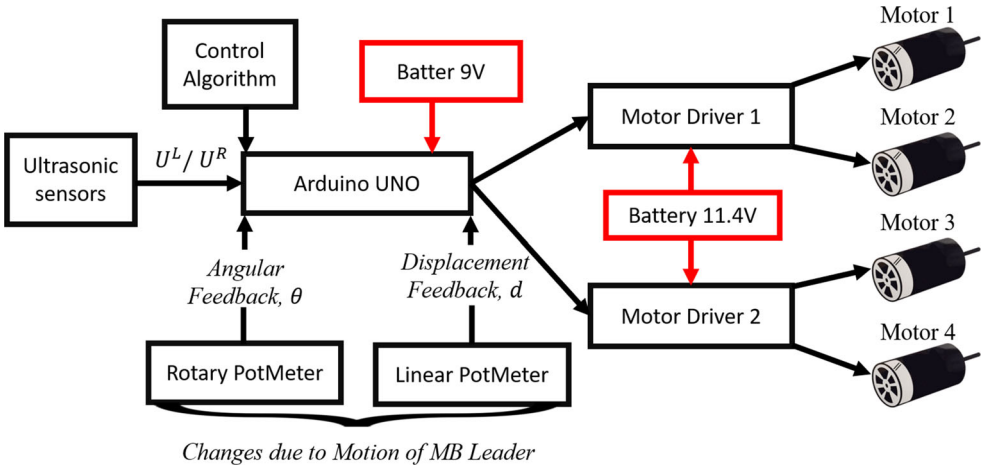

Fig. 8 Control and power layout of follower robot

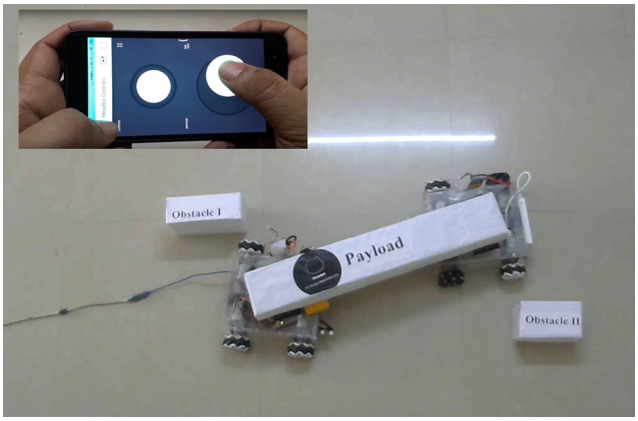

Fig. 9 An operator remotely maneuvering using two analog joysticks(left for orientation and right for translation control) the leader robot through the obstacles as per visual feedback

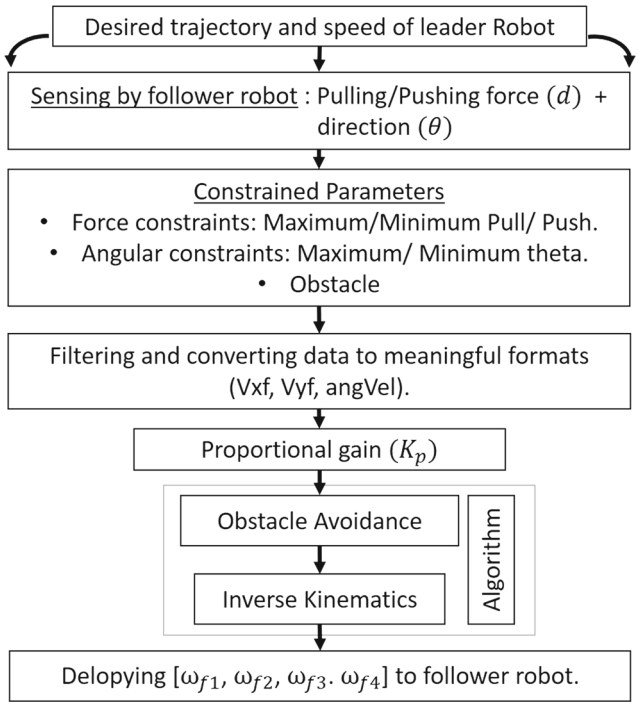

Fig. 11 Sequence and data flow of the overall coordinated manipulation. The command initiates from the leader robot and finishes on the follower robot

Assumption 6 Payload length is assumed to be $> 4L_x$ and has width in the range of the clamping width.

6.2 Problem Formulation

In order to ensure proper functioning of the collaborative strategy, each working case must be analyzed beforehand. With two robots R^L and R^F, the following scenarios are encountered while navigating an environment.

CASE (I), as shown in Fig. 10a, presents two robots, R^L and R^F, in an obstacle-free environment. The (V_{xf}, V_{yf}) and (V_{xl}, V_{yl}) represent the follower and leader robot's velocity along the robot's X_R and Y_R coordinate axis, respectively. During the R^L's motion, a force $\overrightarrow{F}$ is produced on R^F, whose magnitude directly relates to displacement" and the direction is given by "θ". (ω_{f1}, ω_{f2}, ω_{f3}, ω_{f4}) represents the wheel velocity in rad/s for respective wheels, as shown.

CASE (II) is a simple obstacle containing environment. It contains an object on the other side of the R^L. For instance, during initialization of **F** from θ direction, an obstacle is present in the -θ side of R^L as shown in Fig. 10b.

CASE (III) is also an obstacle containing environment. It contains an object on the same side of the R^L, contrary to CASE II. For instance, during initialization of **F** from θ direction, an obstacle is present in the θ side of the R^L, as shown in Fig. 10c.

CASE (IV) is a full-edged obstacle-clustered environment with a combination of CASE II and CASE III, as shown in Fig. 10d. In this case, at a particular interval of

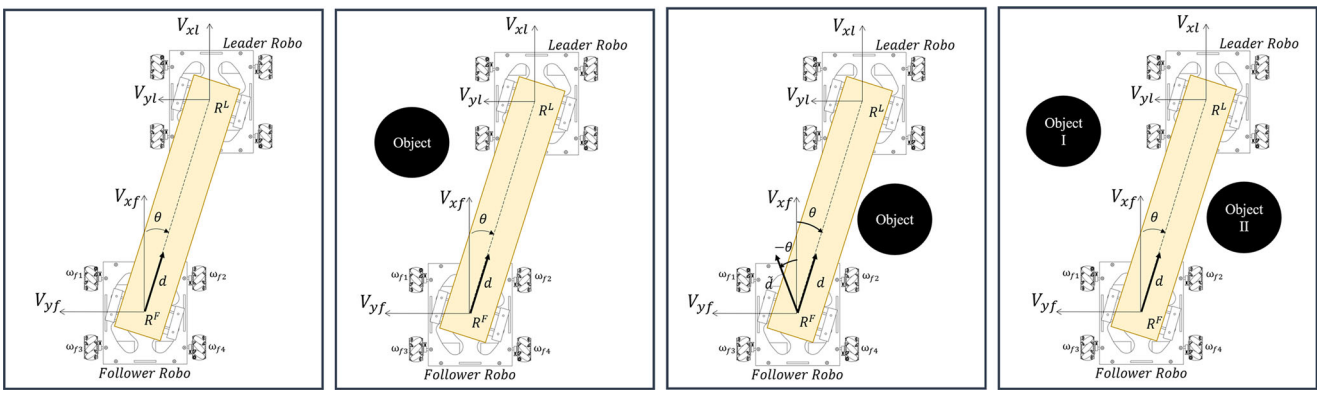

Fig. 10 Various environmental cases under which the collaborative manipulation is formulated upon. Case I, is an obstacle-free environment, whereas cases II, III and IV are obstacle containing environment. Case IV is a combination of Case II and III

time, CASE IV is categorized into either CASE II or III and handled as such consequently.

6.3 Coordination Architecture

Figure 11 describes the coordination architecture between the leader and the follower. A user controls the leader robot where a payload is clamped on it as well as on the follower robot in such a way that there is no relative motion between any of the clamps and the payload. Whenever the leader robot moves, the payload moves along with it, producing forces on the follower robot. The follower robot senses the force as per the degree of displacement produced "d (scalar quantity) and direction along the force by "θ.". Additionally, the follower robot senses it if an obstacle is present on its forward-right and forward-left positions. These readings are checked to the working range of the algorithm deployed in the follower robot; if not met, certain values viz. ω_z are added. The dataset are is filtered and converted to a meaningful format (e.g. $[V_{xf}, V_{yf}, \omega_z]$) which is proportionally amplified with a constant Kp. If the data received does not fall into its range, a different set of operation is performed, if needed (e.g., Obstacle Avoidance). Finally, ($[V_{xf}, V_{yf}, \omega_z]$) are converted to $(\omega_{f1}, \omega_{f2}, \omega_{f3}, \omega_{f4})$ through an Inverse kinematic Equation 2, this contains the individual rpm required by each wheel to achieve the desired outcome and is hence uploaded to the respective motors.

6.4 Control Algorithm

Algorithm 1 Updating (R_F)Follower Robot's position.

```
function UpdateManipulation(d, θ, U_L, U_R)
  IF θ > 0 AND U_L==TRUE
    OR θ < 0 AND U_R==TRUE THEN
      θ ← −θ
  ENDIF
  (V_xf, V_yf, ω_zf) ← (4, 5, 6)
  (ω_f1, ω_f2, ω_f3, ω_f4) ← (2)
```

Figure 12 and Algorithm 1 describes the flow of command taking place in the follower robot with the attributes driven from leader robot and its local environment. The follower robot's (R^F) algo.1. deployed in the micro-controller as shown in Fig. 12 is designed based on the cases mentioned in Fig. 10. The values received by the left ultrasonic sensor "U^L", right ultrasonic sensor "U^R", linear potentiometer "d" and rotary potentiometer "θ" are input parameters for this algorithm. During cases CASES I and II, the robot moves along $\vec{F}$ using Eq. 2. This is so because "U^L" and "U^R" have no impact on the overall trajectory. Taking case II for instance in Fig. 10b, an obstacle present in another direction where R^F is moving along $\vec{F}$ does not hamper its motion. On the other hand, CASE case III, where an obstacle is present in the vicinity of $\vec{F}$ (either left or right), affects the motion of the R^F. In this case, the algorithm sets the motion at "-θ" direction to perform obstacle avoidance till the instance when there is no obstacle according to CASE case III (either left or right). CASE Case IV being a combination of CASE Case II and CASE Case III scenarios, it uses each of the conditions and their corresponding output to tackle such an obstacle-clustered environment.

7 SIMULINK Model of MeWBot

A Simulink model is created for the follower robot with four Mecanum wheels to understand the various translated trajectories it can accomplish without changing its orientation. The Simscape Multibody Link add-on for SolidWorks exports SLDASM-file to slx-file with each part in STEP format. This uses coordinates of each part in the assembly for defining joints and their position. Hence, proper care is taken to generate only need-based coordinates during its assembly.

Angular speeds of $\omega_1, \omega_2, \omega_3, \omega_4$ is given to each revolute joint of the wheel respectively in rad/s. These speeds are given as input to the "Four-Wheel Mecanum Simulation" found in Mobile Robotics Simulation Toolbox in SIMULINK, as shown in Fig. 13. This block then

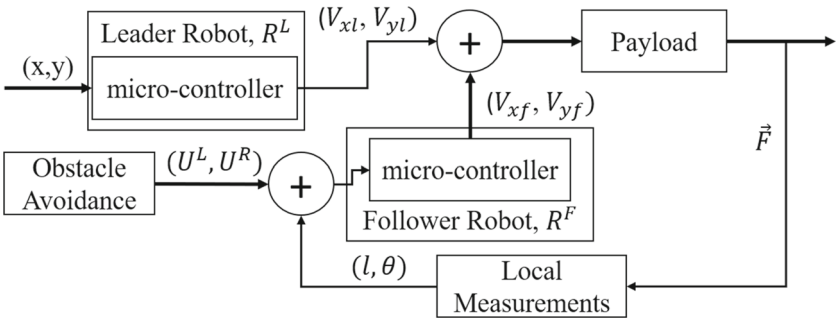

Fig. 12 Overall control system of two-robots: The follower robot is driven based on local measurements (viz. l or d and θ) and an obstacle avoidance technique using U_L and U_R

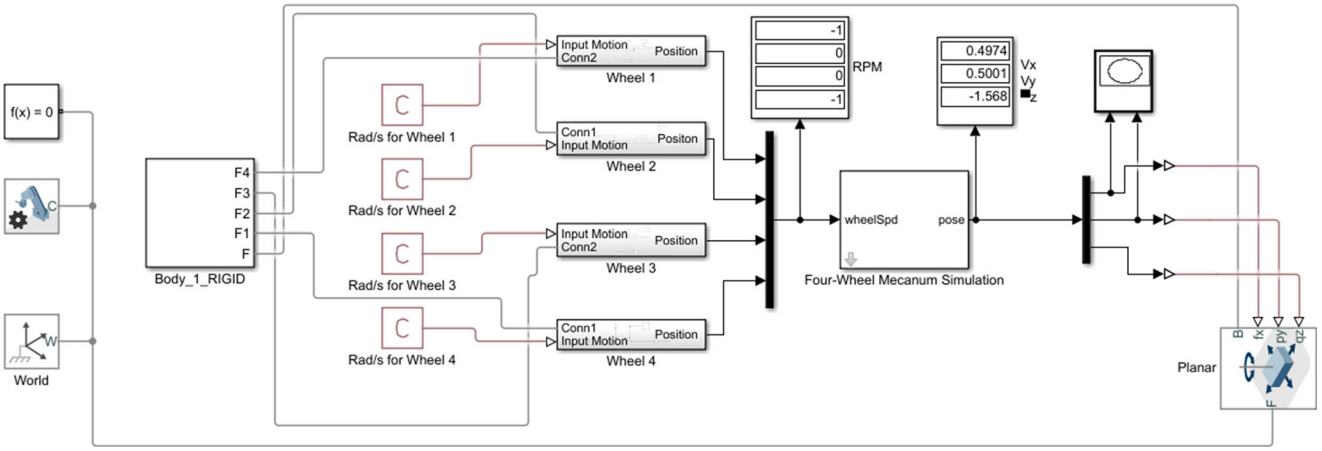

Fig. 13 SIMULINK Model of the proposed robot for kinematic motion analysis

generates (X, Y, θ) defining the robot's position and orientation which are most important parameters for the planar joint.

8 Results for Kinematic Simulation of MewBot

By maintaining the same speed of the wheels at same a particular time, the eight-direction motion of the wheel can be accomplished without changing its operation. The motion of 0° to 360° can be obtained by changing the angular velocities of each wheel, as shown in Fig. 14. For example, to make a transverse motion to the left, the left wheels are rotated against each other in an inward direction and the right wheels are rotated against each other in an outward direction. The different motion cases are given below: -

CASE (a). Motion in a forward direction: Here, the reaction forces on the forward roller act diagonally forward which results into two components - one acting perpendicular to the wheels' motion and other acting towards the wheels' motion. The acting perpendicular forces get cancelled and other motion adds and make forward motion.

CASE (b). Motion in a backward motion direction: Here, the process is like CASE case (a) but the reaction forces act in a backward direction and the add up forces result in backward direction motion.

CASE (c). Motion in the right direction: In this case, the right wheels are rotated against each other in an outward direction while the left wheels are rotated against each other in an inward direction. Ultimately, the desired motion is achieved.

CASE (d). Motion in the left direction: Similarly, in the left direction, the left wheels are rotated against each

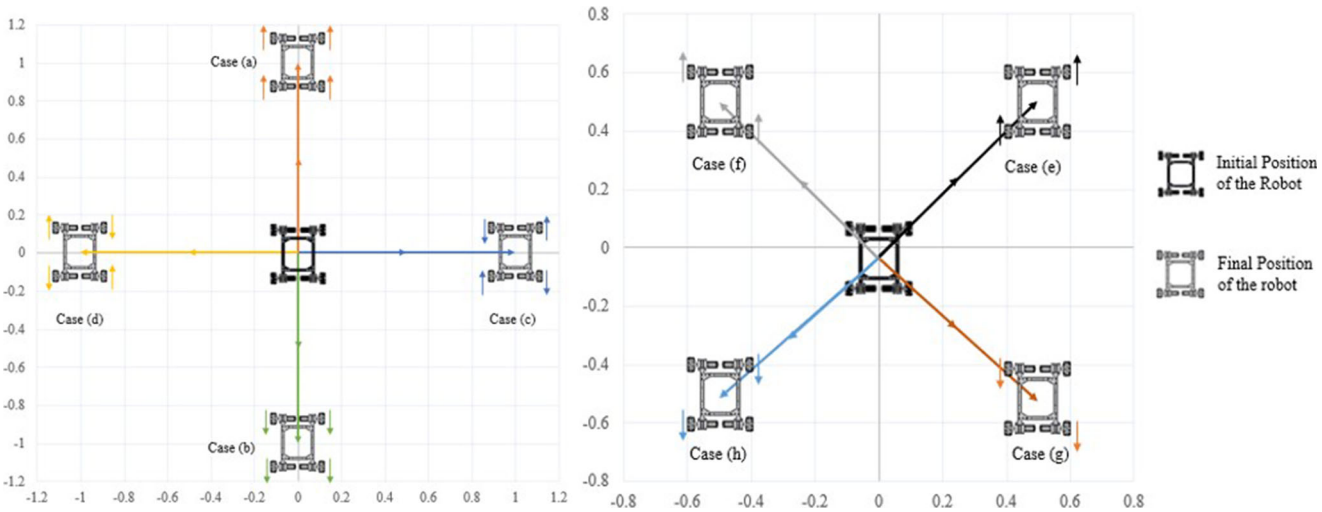

Fig. 14 Kinematic simulation results obtained from SIMULINK platform. The results show the 8 basic trajectories obtained by controlling the wheel speed of each motor. The mecanum wheels are mounted in a diamond-style-configuration during simulation and not the cross

Table 1 Calculated results of forward Kinematics of MewBot using Eq. 1

Cases	Robot velocity			Wheel angular velocity (rad/s) [Calculated]			
	$V_x(m/s)$	$V_y(m/s)$	$\omega(rad/s)$	ω_1	ω_2	ω_3	ω_4
A	1	0	0	26.247	26.247	26.247	26.247
B	−1	0	0	−26.247	−26.247	−26.247	−26.247
C	0	1	0	−26.247	26.247	26.247	−26.247
D	0	−1	0	26.247	−26.247	−26.247	26.247
E	0.707	0.707	0	0	37.1132	37.1132	0
F	0.707	−0.707	0	37.1132	0	0	37.1132
G	−0.707	0.707	0	−37.1132	0	0	−37.1132
H	−0.707	−0.707	0	0	−37.1132	−37.1132	0
I	0	0	1	−6.168	6.168	−6.168	6.168
J	0	0	−1	6.168	−6.168	6.168	−6.168

other in an outward direction while the right wheels are rotated against each other in an inward direction.

CASE (e). Motion in a forward right direction: In this case, the forward right wheels are rotated in the forward direction and wheels' motion is achieved.

CASE (f). Motion in the forward left direction: Here, the forward left wheels rotate in the forward direction to achieve this motion.

CASE (g). Motion in the backward right direction: In this case, the backward right wheels are rotated in the backward direction.

CASE (h). Motion in the backward left direction: In this case, the backward left wheels are rotated in the backward direction.

Figure 14 shows the results obtained from the SIMULINK platform for eight of the basic translation motions that can be obtained without changing the orientation of the robot.

Additionally, Table 1 indicates the calculated results obtained from Eq. 1 and Table 2 referring to the values of individual wheel velocities obtained from the simulation. It can be seen that the equations stated are appropriate and valid with minimal errors. This indicates that the model can be incorporated with the suggested control system to attain the desired trajectory of the MewBot.

9 Experimental Results of Collaborative Manipulation

The manufactured leader and follower robots are subjected to experimental analysis based on the above four environmental cases. A 350g payload made from cardboard with the dimensions $750mm \times 105mm \times 75mm$ is clamped on both the robots such that the distance between each robot's origin is 640mm(approx.). The leader robot is remotely controlled from a location by a user over/using an Internet

Table 2 Simulation results of various motions by MewBot using SIMULINK Model 13

Cases	Robot velocity			Wheel angular velocity (rad/s) [Simulated]			
	$V_x(m/s)$	$V_y(m/s)$	$\omega(rad/s)$	ω_1	ω_2	ω_3	ω_4
A	1	0	0	26.25	26.25	26.25	26.25
B	−1	0	0	−26.25	−26.25	−26.25	−26.25
C	0	1	0	−26.25	26.25	26.25	−26.25
D	0	−1	0	26.25	−26.25	−26.25	26.25
E	0.707	0.707	0	0	37.11	37.11	0
F	0.707	−0.707	0	37.11	0	0	37.11
G	−0.707	0.707	0	−37.11	0	0	−37.11
H	−0.707	−0.707	0	0	−37.11	−37.11	0
I	0	0	1	−6.168	6.168	−6.168	6.168
J	0	0	−1	6.168	−6.168	6.168	−6.168

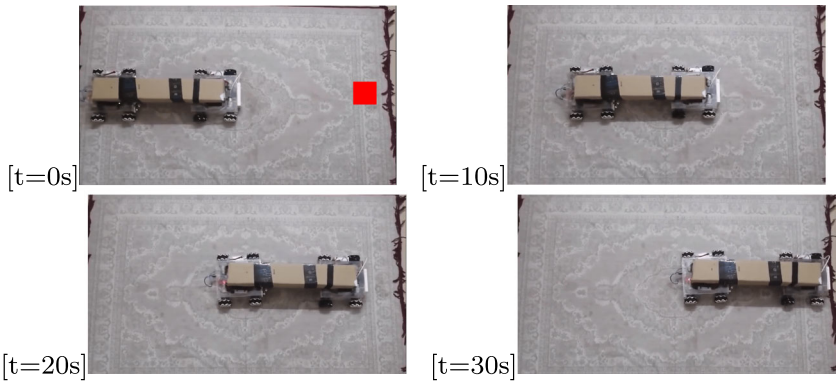

Fig. 15 Outcome of the leader robot(right) guiding the follower robot(left) along a straight line

connection. The site of the experiment is the same but the surface on which the robot moves is changed depending on the range of data to be collected or to improve traction between the wheels and platform by using a carpet. The above-mentioned assumptions are considered during the experimental analysis. During the analysis, we have considered above mentioned assumptions during these experiments. The displacement, theta and calculated individual wheel velocities are recorded at 10Hz and saved for analysis after the completion of the task. All the data collected is initially from the robot's rest position and can also be seen in the graph. Moreover, the videos are captured using a 720p Logitech camera. Snapshots are taken particular intervals to properly visualize the trajectory covered by each robot. To maintain the study's criterion, these robots run the same program for all the above-mentioned cases be running the same program over the following mentioned cases.

These experiments are conducted purely to showcase the feasibility of displacement-based-force sensing collaborative strategy and the added benefits of maneuverability with omni-directional robots under various obstacle-clustered scenarios. The displacement -based force sensing can be understood as a magnitude of displacement of payload on the follower robot when the clamped payload experiences a pull force from the leader robot. Here, the second order derivative of displacement(d) with respect to time is in direct correlation to the magnitude of the pull-force(F).

The red-square in the image of each experiment's initial position denotes the final position of the leader robot. The exact position of the follower robot along-with is uncertain to predict as it depends on the dynamic environment and the obstacles (Fig. 15).

9.1 CASE I(a): Leader and Follower Robot Moving Along a Straight Path

This test is done to initially understand the displacement-based force sensing mechanism put underneath the follower robot. In this experimental scenario, the user remotely controls the leader robot along a straight path on the carpet. The follower robot senses this pull force through the payload using on-board sensors (i.e. purely relying on local measurements), and proportionally moves in a direction towards the force. To ensure that the follower robot is actually contributing to the collaborative manipulation, a graph is plotted between displacement due to the force sensed through the slide potentiometer versus time, as shown in Fig. 16a. Furthermore, the theta vs time graph

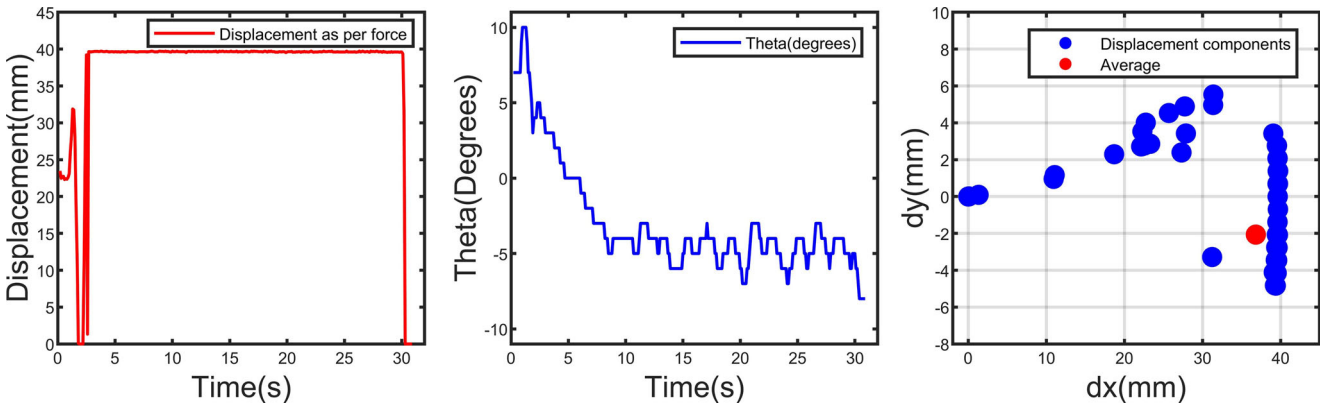

Fig. 16 [From left] Results obtained while performing experiment on Case I.a. **a** Displacement measures, **b** Changes in theta(θ) and **c** Displacement component histories on $X_R O Y_R$ coordinate in follower robot's motion from the leader robot's guiding force during the experiment

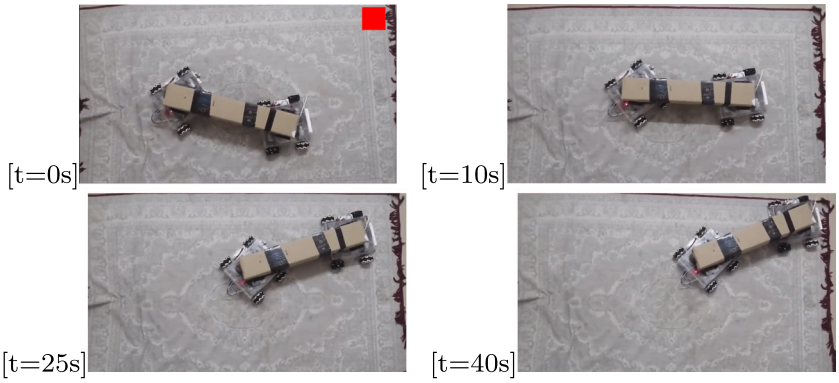

Fig. 17 Outcome of the leader robot(right) guiding the follower robot(left) through a curve path

depicted in Fig. 16b, indicates that theta fluctuates most of the time due to noise and friction between the clamp slides on the follower robot, and maintains an overall angle. Additionally, from Fig. 16c, the displacements at a particular interval of time "t" can be noted. The values are scattered all over due to noise and disturbances in the process. Also, it is assumed that moving in a straight path will not include the d_y component resulting in the average to fall on the line $d_y = 0$ but it is due to noise that a mean value of (36.83, -2.1) is obtained with -2.1 indicating an error value (Fig. 17).

9.2 CASE I(b): Leader and Follower Robot Moving Along a Curvy Path

This experiment is an extension to Case I(a), meaning, the robots are put through a similar obstacle-free environment with the same platform to roll upon, the difference being that these robots perform a curved motion instead of following a straight path. This experiment is done to showcase the fact that irrespective of the position or the source of the leader robot, the follower robot maneuvers towards the applied force using Eq. 2. The leader robot is remotely controlled by an operator through Blynk App over an Internet connection and uses visual feedback for position and orientation alignments. It can be seen in the video that despite the orientation changes of the payload placed on the robots, R_F moves along **F** with minimal change in its orientation in the world frame. Moreover, during the experiment, the leader robot starts from a position such that the total change in θ throughout the test is much higher. This is also the reason behind the scattered plot of displacement histories, as seen in Fig. 18c. This experiment also displays the experimental workings of exponentially dependent ω_Z presented in Eq. 6 (Fig. 19).

9.3 CASE II: Obstacle on the Other Side of F

This is the foremost experiment conducted in an obstacle containing environment. The site is the same but to collect more data, so as to fully evaluate the functioning of the deployed algorithm, the carpet is removed and the robot is permitted to run on the tiles. Consequently, it is predicted that disturbances due to wheel slip are likely to occur, amplifying the noise during the manipulation. However, this is the case only with the sensor measuring the magnitude of **F**, i.e. the slide potentiometer: measuring displacement as per the pull for from the leader robot. The angular position

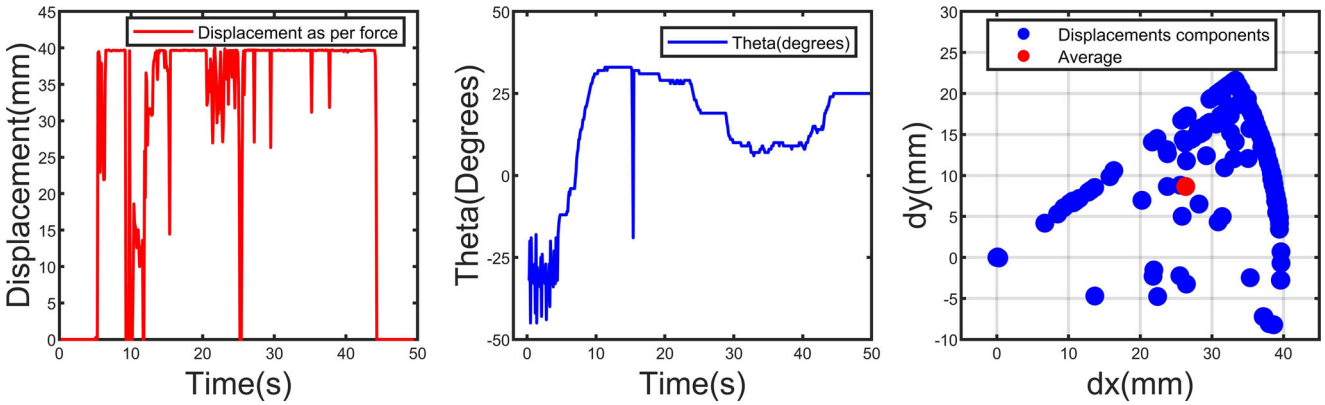

Fig. 18 [From left] Results obtained while performing experiment on Case I.b. **a** Displacement measures, **b** Changes in theta(θ) and **c** Displacement component histories on $X_R O Y_R$ coordinate in follower robot's motion from the leader robot's guiding force during the experiment

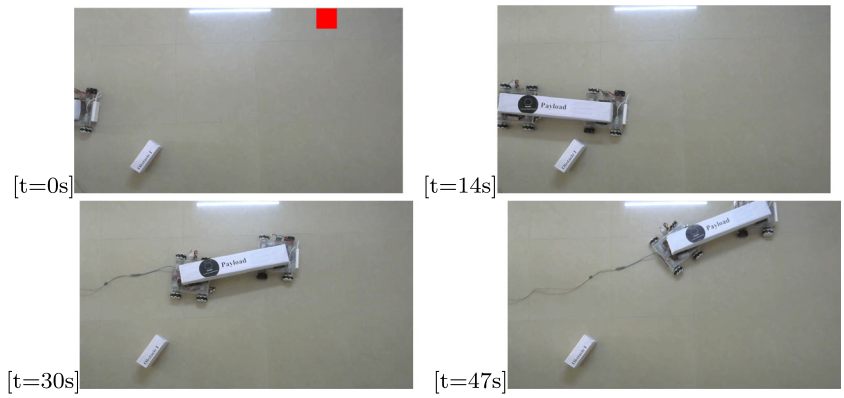

Fig. 19 **a**-**d** displaying the trajectory covered by the leader robot(right) and the motion computed by the follower robot(left) satisfying the conditions of Case II

θ and ultrasonic sensors (U^L, U^R) are not quiet and are affected due to this change of parameter. Hence, an analysis is done considering the aforementioned conditions (Fig. 21).

As per case II, an obstacle I is placed on the right side of the leader robot (R^L). The operator, as per visual information, commands the leader robot to move towards a forward left path just grazing the obstacle so that the follower robot senses the coming obstacle using ultrasonic sensors. This experiment displays the extent of incorporating obstacles in its (R^F's) trajectory, in this case it is $NULL$. In other words, if R^F follows **F**, it will ultimately avoid the obstacle in this case; therefore, the algorithm neglects making any changes to R^F's motion due to the obstacle. To point out the data collected when the R^F senses an obstacle, a grey window is assigned, as seen in the graph shown in Fig. 20, i.e. between $t = 11s$ and $t = 16.8s$. This data indicates that despite an obstacle sensed by the right ultrasonic sensor, the rate of change of θ is not sudden, i.e. $d\theta/dt$ at $11s \leq t \leq 16.8s$ is equal to $0.3448°/s$. A high $d\theta/dt$ would indicate that the follower robot moves away from an obstacle when following **F** which would ultimately lead to collision. Also, for validating the effectiveness of the manipulation, the displacement-based-force-feedback sensed by the follower robot is shown in Fig. 20c.

9.4 CASE III: Obstacle on the Same Side of F

This is another experiment conducted in an obstacle environment. The site is the same along with the same surface conditions as in CASE II. Here, the obstacle position with respect to the leader is opposite to that of CASE II, i.e., the obstacle is present on the same side of **F**. It is different from the previous case as during manipulation, if the follower unavoidably moves towards **F** then a collision is likely to take place. Therefore, the obstacle detected is to be a parameter in the motion algorithm. R^L is guided by an operator such that the leader robot moves right beside and comes in front of the obstacle. The R^F may hit the obstacle, if not sensed and avoided intime. The time at which the R^F senses an object is marked by a grey window, as shown in Fig. 22.

As per case III, an obstacle I is kept to the right of the leader robot. The operator controls R^L remotely and maneuvers through the given set of protocols using visual feedback. During this task, the follower robot senses an obstacle on its forward-right position and instead of moving in θ direction (i.e. towards **F**), the follower robot moves in -θ direction to negate the change and avoid a collision with the obstacle. Due to this, a high $d\theta/dt$ takes place

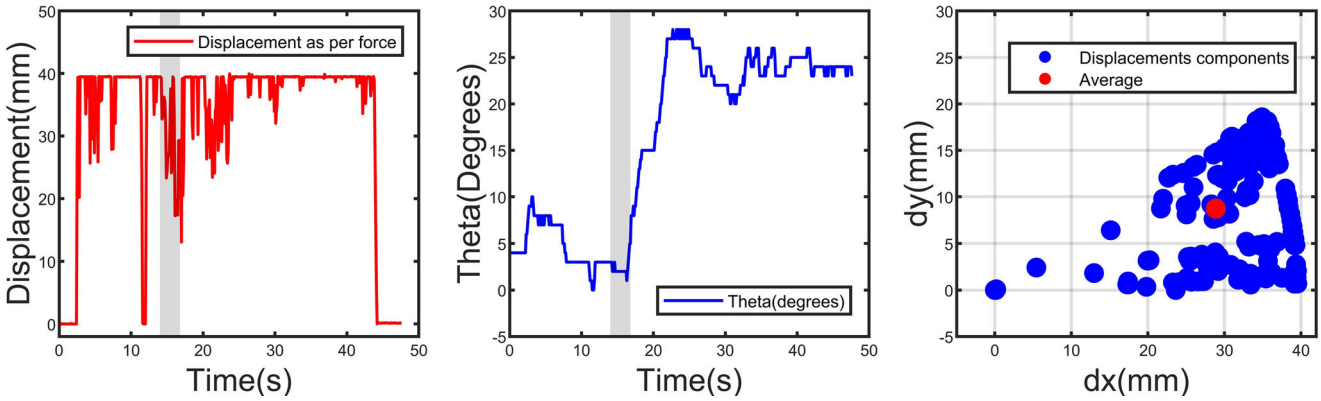

Fig. 20 [From left] Results obtained while performing experiment on Case II. **a** Displacement measures, **b** Changes in theta(θ) and **c** Displacement component histories on $X_R O Y_R$ coordinate in follower robot's motion from the leader robot's guiding force during the experiment

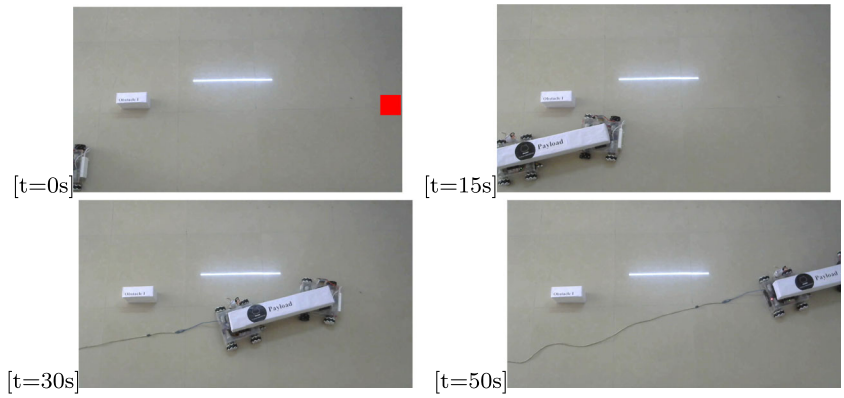

Fig. 21 **a**-**d** displaying the trajectory covered by the leader robot(right) and the motion computed by the follower robot(left) satisfying the conditions of Case III

during this instant of time. It can be seen in Fig. 22b, that an obstacle is detected during t = 10:6s and t = 16:1s, during which the value of $d\theta/dt$ is $1.4545°/s$. It is evident that the chosen algorithm is versatile and is able to choose when to perform what action depending on the environmental conditions. Furthermore, the displacement-based force feedback is plotted using the experimental data set, as seen in Fig. 22c. The overall task is not very smooth as the human operator has to visually control the leader robots' motion based on the conditions of the experiment (Fig. 23).

9.5 CASE IV: Crowded Environment

This is the final test which can fully validate the present study's collaborative manipulation in an obstacle-clustered environment. The condition is an amalgamation of both CASE II and CASE III, i.e., an obstacle is located both at R^L's forward-right and forward-left positions one after the other. This will not only cross verify the results obtained in each of these cases individually but also show that the deployed algorithm is suitable for an obstacle containing environment. In this scenario, the algorithm will categorize each obstacle-sensed-period-of-time between either CASE II or CASE III, making it easier for the follower robot to maneuver through the obstacles, without any ambiguity.

Satisfying the conditions, two obstacles, i.e., obstacle I and obstacle II are placed in the forward-left and forward-right directions of the leader robot, respectively. The operator navigates the leader robots through these obstacles with visual feedback. Each of these interactions is categorized into two stages, as indicated by two grey windows in Fig. 24. R^F's first interaction is with obstacle I, with **F** pointing to the same side as the obstacle, categorising it to be CASE III on its first interaction. The obstacle is sensed between time $t = 14s$ and $t = 21.8s$, making $d\theta/dt$ to be $1.923°/s$. $d\theta/dt$ at interval $14s \leq t \leq 21.8s$ is high which verifies that the follower executed the avoidance algorithm and steered clear from any collision during this time period. Moving ahead, during the follower robot's interaction with obstacle II, the **F** is in the other direction to that of the position of the second obstacle. Therefore, the second stage is categorized into CASE II, in which the follower robot's trajectory is independent of the obstacle position specially in the other side of **F**. As seen in Fig. 24b, in the second grey window(i.e. when $37.6s \leq$

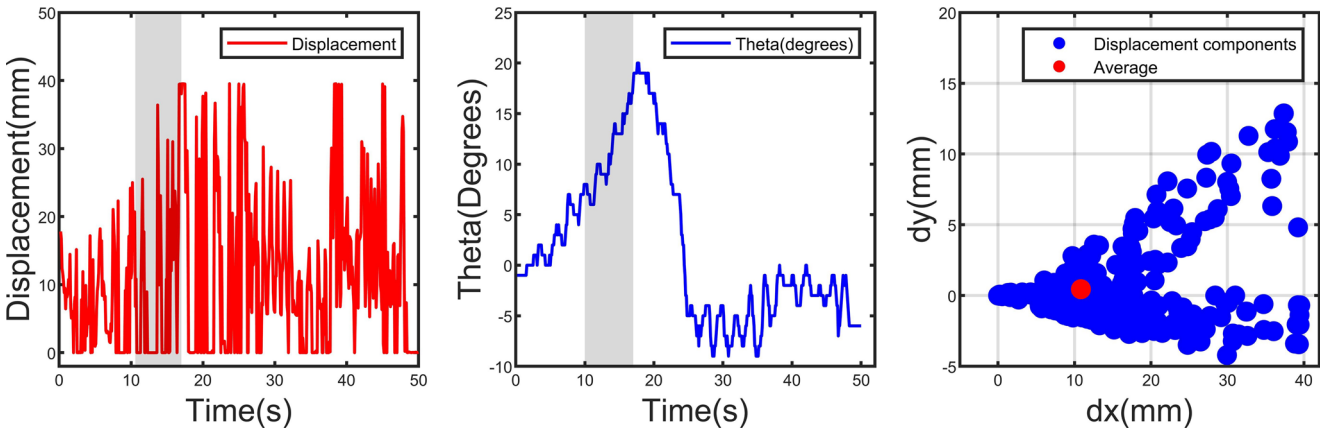

Fig. 22 [From left] Results obtained while performing experiment on Case III. **a** Displacement measures, **b** Changes in theta(θ) and **c** Displacement component histories on $X_R O Y_R$ coordinate in follower robot's motion from the leader robot's guiding force during the experiment

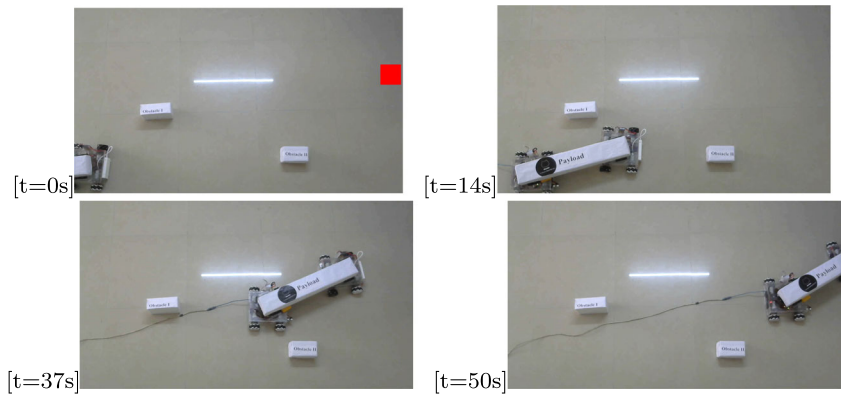

Fig. 23 **a**–**d** displaying the trajectory covered by the leader robot(right) and the motion computed by the follower robot(left) satisfying the conditions of Case IV

$t \leq 40.1s$), the value of $d\theta/dt$ is $0.4°/s$, which conveys that the follower robot's trajectory is independent of the position of Obstacle II. Moreover, as the leading system is human-operated, the overall motion is not very smooth, due to which the displacement histories by R^L to R^F are a bit scattered, as seen in Fig. 24c.

10 Conclusion and Future Work

The project presents a displacement-based collaborative strategy using one leader and follower robots in an obstacle-clustered environment. The leader robot is manually controlled from a remote location using Wi-Fi connectivity whereas the follower robot is pushed to full autonomy using appropriate sensors to gather the required local measurements. A payload falling in the range of the study's experimental requirement is clamped on both the leader and follower robots with the stated assumption 2. To maneuver easily through narrow paths, four Mecanum-Wheeled Robots (MeWBot) are considered, due to their ability to provide translation in 360° direction without changing their orientation. In collaborative operation, the robots use no explicit communication and solely depend on the implicit information received through payload movement-producing-forces. A control algorithm is deployed in the follower robot to analyze these forces. These are sensed in terms of displacement as a function of the force's magnitude and direction with separated on-board sensors. The algorithm is integrated with an obstacle avoidance technique to perform a coordinated task in a complex (obstacle-contained) environment.

The results from the motion analysis simulation show that the four Mecanum wheeled robots perform full omni-directional motion. The forward and inverse kinematic results are obtained using a SIMULINK model which shows that the Mecanum wheel in this platform can move from 0° to 360° in any direction without changing its orientation. Also, these results are compared with the calculated ones and they are found to converge with minimal error. With this knowledge, an experimental set-up is prepared with the required hardware and test environments to validate the proposed strategy of collaborative manipulation. The results from this experimental investigation indicate that the leader and follower robots produce a synchronous motion with the shared payload. The omni-directional

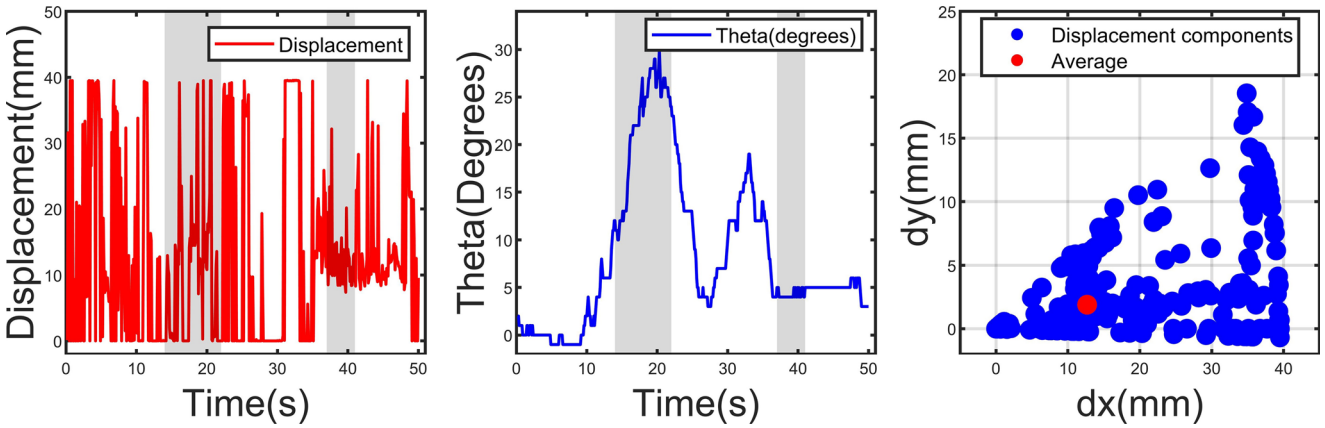

Fig. 24 [From left] Results obtained while performing experiment on Case IV. **a** Displacement measures, **b** Changes in theta(θ) and **c** Displacement component histories on $X_R O Y_R$ coordinate in follower robot's motion from the leader robot's guiding force during the experiment

capability of the mounted Mecanum wheels provides an unconstrained motion which is appropriate for use in the stated environmental conditions.

As an advancement in the current project, it is at-most important to address the overshoots and oscillation seen on the follower robot due to a proportionally-driven controller, and, this can be achieved with further research on the adaptive-movement control system. Also, to reduce the uncertainty and make the system more reliable - effective filtering and modulating techniques like Kalman filter can be applied to properly validate sensor readings. Though we see that the current micro-controller is limited by many attributes - instead of upgrading and installing more costlier controllers, a better alternative of cloud robotics can be opted. Coming to the enhancements on hardware, due to wheel slip and the need to reduce assumptions as much as possible (particularly assumption 5), an individual suspension system is to be modelled on each wheel depending on the nature of the floor surface it is to be tested upon. Furthermore, to achieve an effective SLAM technique, LiDAR sensor can be made on-board. The proposed methodology can be tested for coordination between a greater number of robots, i.e., one leader and more than one follower robot.

Supplementary Information The online version contains supplementary material available at https://doi.org/10.1007/s10846-021-01359-5 .

Acknowledgements This investigative research work was supported by SRMIST, Chennai. The authors would like to convey their immense gratitude to Mr. Binay Kumar Mahato, Mr. Prabin Bhandari, SRM Fab Lab and SRM Team ROBOCON for the help rendered during the course of this study.

Author Contributions All authors contributed to the study conception and design. The model preparation and kinematic simulation was performed by Aditya Rauniyar and Aman Mishra. Material preparation, data collection and analysis were performed by Aditya Rauniyar and Hem Chandra Upreti. The first draft of the manuscript was written by Aditya Rauniyar and all authors commented on previous versions of the manuscript. All authors read and approved the final manuscript. Supervision on the overall project was led by Prabhu Sethuramalingam.

Declarations

Competing interests The authors declare that they have no known competing financial interests or personal relationships that could have appeared to influence the work reported in this paper.

References

1. Adamov, B.I.: Influence of mecanum wheels construction on accuracy of the omnidirectional platform navigation (on example of KUKA youBot robot). In: 2018 25th Saint Petersburg International Conference on Integrated Navigation Systems (ICINS). St. Petersburg, Russia, 28-30 May (2018)
2. Adăscăliţei, F., Doroftei, I.: Practical applications for mobile robots based on mecanum wheels-A systematic survey. In: The Romanian Review Precision Mechanics, Optics and Mechatronics (2011). B-dul D. Mangeron, 61-63, 700050 Iasi, Romania
3. Alonso-Mora, J., Knepper, R., Siegwart, R., Rus, D.: Local motion planning for collaborative multi-robot manipulation of deformable objects. In: IEEE International Conference on Robotics and Automation (ICRA) Washington State Convention Center Seattle, Washington, pp. 26–30 (2015)
4. Amanatiadis, A., Henschel, C., Birkicht, B., Andel, B., Charalampous, K., Kostavelis, I., May, R., Gasteratos, A.: An autonomous multi-robot system for vehicle extraction and transportation. In: IEEE International Conference on Robotics and Automation (ICRA) Washington State Convention Center, Seattle, Washington, pp. 26–30 (2015)
5. Amato, C., Konidaris, G., Cruz, G., Maynor, C.A., How, J.P., Kaelbling, L.P.: Planning for decentralized control of multiple robots under uncertainty. In: 2015 IEEE International Conference on Robotics and Automation (ICRA) Washington State Convention Center Seattle, Washington, vol. 2015, pp. 26–30 (2015)
6. Baldassarre, G., Trianni, V., Bonani, M., Mondada, F., Dorigo, M., Nolfi, S.: Self-organized coordinated motion in groups of physically connected robots. IEEE Trans. Syst. Man Cybern. (2007)
7. Berman, S., Lindsey, Q.: Mahmut Selman Sakar. Study of Group Food Retrieval by Ants as a Model for Multi-robot Collective Transport Strategies Proceedings of the IEEE, Sept, Vijay Kumar and Pratt, S (2011)
8. Chen, J., Gauci, M., Gross, R.: A strategy for transporting tall objects with a swarm of miniature mobile robots. In: 2013 IEEE International Conference on Robotics and Automation (ICRA), Karlsruhe, Germany, May 6-10 (2013)
9. Culbertson, P., Schwager, M.: Decentralized adaptive control for collaborative manipulation. In: IEEE International Conference on Robotics and Automation (ICRA) Brisbane, QLD, Australia (2018)
10. Doroftei, I., Grosu, V., Spinu, V.: Omnidirectional mobile robot – design and implementation. In: IEEE International Conference on Mechatronics and Automation (ICMA), Takamatsu, Japan, 24 August (2007)
11. Erhart, S., Sieber, D., Hirche, S.: An impedance-based control architecture for multi-robot cooperative dual-arm mobile manipulation. In: IEEE/RSJ International Conference on Intelligent Robots and Systems (IROS), November 3-7, Tokyo, Japan (2013)
12. Esposito, J.M.: Decentralized cooperative manipulation with a swarm of mobile robots: the approach problem. In: American Control Conference Marriott Waterfront, Baltimore, MD, USA, June 30-July, 02 (2010)
13. Fink, J., Hsieh, M.A., Kumar, V.: Multi-robot manipulation via caging in environments with obstacles. In: IEEE International Conference on Robotics and Automation Pasadena, CA, USA, May, 19–23 (2008)
14. Franchi, A., Petitti, A., Rizzo, A.: Decentralized parameter estimation and observation for cooperative mobile manipulation of an unknown load using noisy measurements. In: IEEE International Conference on Robotics and Automation (ICRA) Washington State Convention Center Seattle, Washington, May, 26–30 (2015)
15. Teixeira, M.A., Santos, H.B., de Oliveira, A.S., Fabro, J.A., de Arruda, L.V.R., Neves, F. Jr..: Cooperative load transport based on fuzzy logic controllers. In: IEEE International Conference on Industry Applicartions, Curitiba, Brazil, Nov, 20–23 (2016)

16. Gfrerrer, A.: Geometry and kinematics of the Mecanum wheel. Comput Aid Geometr Des **25**(9), 784–791 (2008)
17. IIon, B.E.: Wheels for a course stable self-propelling vehicle movable in any direction on the ground or some other base. (patent Sweden) B60B 19/12 (20060101); B60b 019/00, REF/3876255, November 13 (1972)
18. Chen, J., Gauci, M., Li, W., Kolling, A., Gros, R.: Occlusion-based cooperative transport with a swarm of miniature mobile robots. IEEE Trans Robot **31**(2) (2015)
19. Feng, K.-H.: Fuzzy sliding-mode consensus formation control of networked heterogeneous mecanum-wheeled multi-robots with dynamic effects. IEEE Trans. Syst. Man. Cybern. B Cybern. (2018)
20. Knepper, R.A., Layton, T., Romanishin, J., Rus, D.: IkeaBot: an autonomous multi-robot coordinated furniture assembly system. In: IEEE International Conference on Robotics and Automation (ICRA) Karlsruhe, Germany, May, 6–10 (2013)
21. Li, T., Zhang, J.-F.: Consensus conditions of multi-agent systems with time-varying topologies and stochastic communication noises. IEEE Trans. Autom. Control **55**(9) (2010)
22. Padgett, S.T., Browne, A.F.: Vector-based robot obstacle avoidance using LIDAR and Mecanum Drive. SoutheastCon, Charlotte, NC, USA, 11 May (2017)
23. Pedersen, M.R., Nalpantidis, L., Andersen, R.S., Schou, C., Bøgh, S., Krüger, V., Madsen, O.: Robot skills for manufacturing: From concept to industrial deployment. Robot. Comput. Integr. Manuf. **37**, 282–291 (2016)
24. Song, P., Kumar, V.: A potential field based approach to multi-robot manipulation. In: IEEE International Conference on Robotics and Automation (Cat. No.02CH37292), vol. 2, pp. 1217–1222. IEEE (2002)
25. Röhrig, C., Heß, D.: OmniMan: an omnidirectional mobile manipulator for human-robot collaboration. In: The International MultiConference of Engineers and Computer Scientists, IMECS, Hong Kong, pp. 13–15 (2019)
26. Rus, D., Donald, B., Jennings, J.: Moving furniture with teams of autonomous robots. In: IEEE/RSJ International Conference on Intelligent Robots and Systems. Human Robot Interaction and Cooperative Robots, vol. 1, pp. 235–242. IEEE Comput. Soc. Press (1995)
27. Sadjadi, H., Jarrah, M.A.: Autonomous cleaning system for Dubai international airport. J. Franklin Inst. ,112–124 (2011)
28. Shahin, S., Sadeghian, R., Sedigh, P., Masouleh, M.T.: Simulation, control and construction of a four mecanum-wheeled robot. In: 2017 IEEE 4th International Conference on Knowledge-Based Engineering and Innovation (KBEI) (2017)
29. Taheri, H., Qiao, B., Ghaeminezhad, N.: Kinematic model of a four mecanum wheeled mobile robot. Int. J. Comput. Appl. (0975–8887) **113**(3) (2015)
30. Voinescu, A., Dragomir, D., Draghici, A., Bara, P.: Multiprocessor architecture for a versatile autonomous robot. In: 2nd International Conference on Systems and Computer Science (ICSCS), Villeneuve d'Ascq, France, pp. 26–27 (2013)
31. Wang, Z., Schwager, M.: Force-Amplifying N-robot Transport System (Force-ANTS) for cooperative planar manipulation without communication. Int. J. Robot. Res. **35**(13), 1564–1586 (2016)
32. Wang, Z., Yang, G., Su, X., Schwager, M.: OuijaBots: omnidirectional robots for cooperative object transport with rotation control using no communication. In: Distributed Autonomous Robotic Systems, pp. 117–131 (2018)
33. Zhang, Y., Tian, Y.-P.: Consensus of data-sampled multi-agent systems with random communication delay and packet loss. IEEE Trans. Automat. Control **55**(4) (2010)

Aditya Rauniyar received his B.Tech in Mechanical Engineering from SRM Institute of Science and Technology (SRM IST), India in 2019 and has 3 years of experience in designing, developing, programming and testing robotic solutions. He has worked as a Research Assistant at BBRC and IIT Madras, India and is currently working as a Software Engineer under an IIOT domain. Aditya was awarded with full scholarship to pursue his B.tech where, as of date, has filed a patent in V2 Pneumatic Engine and has authored IEEE ICCIC'18 - achieving a best paper award. He is also awarded with the best project from his batch during this pursuit. His research interest includes but is not limited to Collaborative manipulation, Cloud robotics and Computational Motion Planning.

Hem Chandra Upreti received a BE in Mechanical Engineering from SRM Institute of Science and Technology, Chennai (India) in 2019. He had an industrial experience of 1 years as Production Engineer. He has also worked as Research coordinator of Society of Mechanical Engineers Nepal. His topic of interest includes Design, Robotics, Vibration and Simulation. Currently working on "Design and Simulation of advance solar food drying including PCM".

Aman Mishra received a B. Tech in Mechanical Engineering from SRM Institute of Science and Technology, Chennai, India in 2019, currently pursuing M. Tech in Design Engineering from Indian Institute of Technology (IIT), Bombay, India. He had also worked in Autonomous underwater vehicle (AUV), a tech team during college. He had also worked as Vice-chairperson of American Society of Mechanical engineers (ASME) for 3 years during B. Tech. Also, He presented conference paper on Numerical simulation of supersonic film cooling at high enthalpy condition. He had an industrial experience of around 8 months as Production Engineer. He is currently working on "Gaits and stability Analysis of Four-Legged Robot" as research topic. His topic of interest includes vibration, Robotics, static and dynamic system and topic related to this.

Prabhu Sethuramalingam received a BE in Mechanical Engineering from Bharathiar University, India in 1996, ME in Production engineering from Madurai Kamaraj University in 2000, and currently working as Professor in the Department of Mechanical Engineering, SRM Institute of Science and Technology, Chennai(India). He had an industrial experience of 4 years as Production Engineer and 20 years of teaching and research experience. He has won the Best teacher award and the Best project award. He is the author of 74 international journal papers, 33 International conferences and 20 National conference papers and 3 patents were published and 2 patents were filed. His research interest includes nanotechnology, nanomachining, Expert system, Design of experiments, Nano materials and Robotics. Currently Guiding Five PhD research scholars and one PhD scholar Completed in the field of Carbon nano tube based applications in Cutting tool and Grinding tool and Wire EDM tool, Composite and Robotics and 1 PhD scholar Completed.